Modeling of Macromolecular Alignment in Nematic Virus Suspensions. Application to the Prediction of NMR Residual Dipolar Couplings

Alberta Ferrarini*

Dipartimento di Chimica Fisica, Università di Padova, 2 via Loredan, 35131 Padova, Italy

Received: February 12, 2003; In Final Form: May 9, 2003

The alignment of macromolecules in dilute suspensions of filamentous phages is described in terms of steric and electrostatic contributions; the former are modeled as excluded volume interactions between a viral particle and a macromolecule, and the latter are treated at the mean field level, through the Poisson−Boltzmann equation for the virus surrounded by an ion density. The virus is represented as a uniformly charged rod, whereas the relevant features of the macromolecule, i.e., shape and charge distribution, are explicitly taken into account. As an application, the residual dipolar couplings between ^{15}N and ^{1}H nuclear spins in the Ig-binding domain of streptococcal protein G are calculated, and their dependence on ionic strength and virus dimension or concentration is analyzed. The theoretical predictions enable us to explain the NMR observations reported for this protein.

Introduction

It has been known for a long time that the orientational order of liquid crystal phases can be exploited to probe magnetic interactions that would be averaged to zero in the isotropic phase.[1,2a] The analysis of residual dipolar and quadrupolar couplings of low molar mass solutes in thermotropic liquid crystals has proven to be a valuable tool to investigate torsional potentials with the advantage, with respect to gas-phase techniques, of providing information on the effects of the environment.[1,2b] Only in recent years has the use of liquid crystal solvents been extended to the conformational analysis of macromolecules: proteins,[3−5] nucleic acids,[6,7] and oligosaccharides[8,9] have been investigated. The requirements of aqueous solvents, sufficiently small splittings, and short relaxation times have been met by dissolving the macromolecules in suspensions of anisotropic colloidal particles, which at suitable concentrations can form lyotropic liquid crystal phases (for a recent review see ref 10). The media used for the earliest experiments were suspensions of bicelles, i.e., disk-shaped phospholipid micelles of large diameter.[4,11] Subsequently, also other aligning media have been tried, such as suspensions of filamentous virus particles[12−14] or oriented purple membrane fragments.[15,16] It has been found that not only the degree of alignment, but also its characteristics can be modified by changing the medium. This property turns out to be useful because, if the structure of the macromolecule is assumed to be independent of the medium, the availability of residual dipolar couplings for different alignments provides a set of independent data.[17,18]

A clear understanding of the dependence of the orientational behavior of a macromolecule on the structure of the aligning medium has not been reached, yet. Alignment would be the result of steric repulsions, which are likely to be similar in the various systems, and electrostatic interactions, which, on the contrary, are expected to depend on the features of the colloidal suspension. Such a picture has been suggested by the observation that alignment of a protein in a bicelle suspension is modified by addition of negatively or positively charged dopants.[4,19] Moreover, the alignment tensors measured in suspensions of viral particles and purple membrane fragments, which are strongly charged, are quite different from those found when bicelles are used.[13,16] As a further support of this view, it has been observed that alignment in virus suspensions can be tuned by changing the ionic strength: the differences with respect to bicellar suspensions are gradually reduced when the ionic strength is increased.[14]

We shall take as the test system the Ig-binding domain of streptococcal protein G (henceforth denoted as protein G), for which residual dipolar couplings between ^{15}N and ^{1}H nuclear spins ($^{1}D_{NH}$) in various liquid crystal media have been reported.[13,14] This protein is highly structured, with four β-sheets and one α-helix, and the X-ray structure is conserved when the protein is dissolved in different media. In Figure 1A,B experimental $^{1}D_{NH}$ values are plotted vs residue number: very specific patterns are obtained, which reflect the orientation of the NH bonds with respect to the static magnetic field (and therefore depend on the protein conformation and overall orientation). The results shown in Figure 1A have been derived from NMR experiments in a nearly neutral bicellar solution, in which the orienting mechanism is deemed to be of essentially steric nature. The profile is quite different from those obtained in virus suspensions, which are displayed in Figure 1B. Here, on the contrary, a clear similarity appears between the residual dipolar couplings measured in *fd* and Tobacco Mosaic Virus (TMV), two filamentous viruses with different dimensions and charge density (the characteristics of commonly used viruses are summarized in Table 1). Such results single out the role of the electrostatic interactions present in virus suspensions, and the scarce relevance of the details of the virus structure. Finally, Figure 1C shows the effect of ionic strength on the dipolar couplings measured in suspensions of Pf1 bacteriophage. We can see that when the salt concentration is increased, the magnitude of the residual dipolar couplings diminishes, which is consistent with a reduction of electrostatic alignment due to higher screening of charges. Moreover, no correlation appears between $^{1}D_{NH}$ values measured at very different salt concentrations, and this is in agreement with the presence of two independent orientational mechanisms.[14]

A deeper understanding of the mechanisms underlying orientational order would be helpful for the analysis of NMR spectra and for the choice of the best experimental conditions.

* Corresponding author. E-mail: alberta.ferrarini@unipd.it.

10.1021/jp034366k CCC: $25.00 © 2003 American Chemical Society
Published on Web 07/12/2003

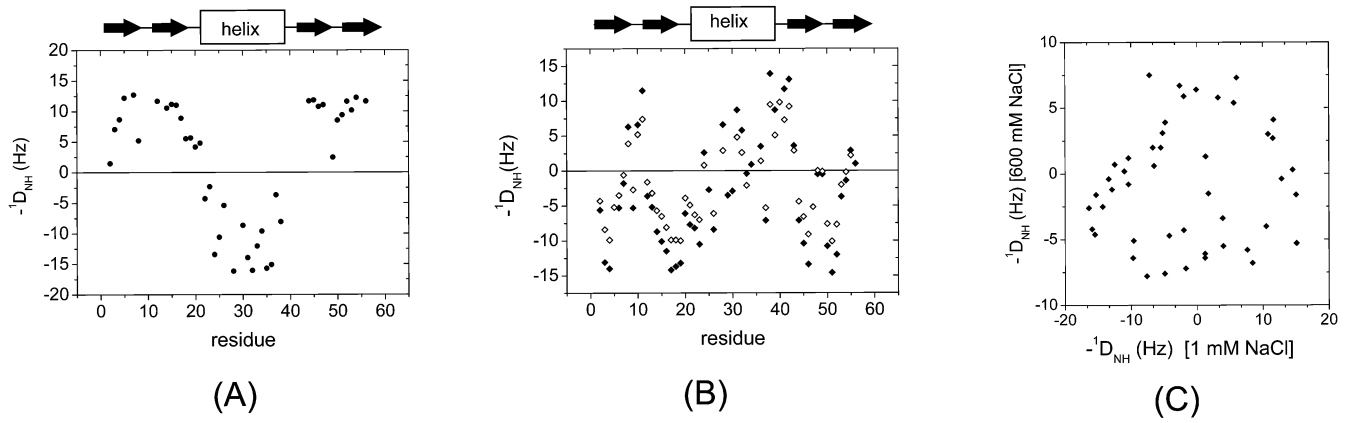

Figure 1. Residual dipolar couplings measured for protein G in different aligning media. (A) Bicelle.[13] (B) (◆) *fd* virus (∼28 mg/mL) and (◇) TMV (∼50 mg/mL), in 50 mM sodium phosphate buffer pH 5.4.[13] (C) Pf1 virus (26 mg/mL) at pH 7.2 and 600 mM NaCl vs 1 mM NaCl.[14]

TABLE 1: Properties of the Filamentous Viruses Considered in This Work

	TMV[22,23]	*fd*[20−22]	Pf1[21,24]
contour length L (nm)	300	880	1900
persistence length P (nm)	>3000	2200	∼2000
diameter D (nm)	18.0	6.7	6.7
molar mass (g mol^{-1})	4×10^7	1.64×10^7	3.75×10^7
linear charge density λ (e nm^{-1})	−20	−10	−10

However, a complete description of the experimental behavior might appear unfeasible, because on one side the NMR oservables depend in a peculiar way on the features of the macromolecule, and this is just the reason for their use for structural investigation, whereas, on the other end, a detailed modeling of the whole system is hindered by its complexity. Filamentous viruses are made of single-stranded DNA or RNA coated with helical proteins and can be sketched as long thin rods, with a high and roughly uniform charge density on their surface. Virions are homogeneously distributed in the sample and, as a consequence of their large length-to-breadth ratio, are highly oriented even at volume fractions of a few percent. For example, in a 30 mg/mL suspension of *fd* bacteriophage (∼0.002 mM) the average distance between rods is about 40 nm and the order parameter is higher than 0.6.[25] Macromolecules, usually at concentrations lower than 1 mM, can have variable size and charge; for a medium-size protein we can expect dimensions on the order of 10 nm and a highly specific charge distribution, with a net charge of some units. As appears from NMR experiments, macromolecules are weakly ordered (order parameter less than 0.001). Finally, the counterions and salt, which have dimensions on the order of tenths of a nanometer and bear charges of one or a few units, are inhomogeneously distributed in the sample, with accumulation of oppositely charged ions and depletion of the equally charged ones in the neighborhood of the polyions.[26] As a consequence of the mutual influence of the various interactions, the whole picture appears to be quite complex.

During the last years there have been several attempts to provide theoretical predictions of macromolecular alignment; however, up to now they have been limited to steric effects. In the model developed by Zweckstetter and Bax[27] the alignment tensor is calculated by averaging over all nonoverlapping configurations of a colloidal particle and a macromolecule. The macromolecular shape is represented with atomistic detail, whereas bicelle and filamentous phages are modeled respectively as an infinite wall and an infinitely long cylinder. Very similar predictions are obtained in the two cases, which are in good agreement with the behavior observed in bicelle based liquid crystals, but cannot explain the results obtained in viral suspensions. Other models, taking into account the macromolecular shape in a less detailed way, have been proposed for the steric alignment: we can remind the parametrization of the alignment tensor according to the gyration[28] or the inertia tensor,[29] or the model for orientation of ellipsoidal particles by planar obstacles.[30] In all cases agreement with measurements in bicelles has been found. Good results can also obtained by using the "surface tensor" approach,[31] which was originally developed for the description of short-range anisotropic interactions in thermotropic liquid crystals.[32] Namely, steric alignment appears to be a property that can be predicted rather well by different models that can somehow take into account the shape of the macromolecule.

On the contrary, not as much has been done for electrostatic interactions, and the prediction of their effects on orientational order is still an open problem. In this work a model for the steric and electrostatic alignment of macromolecules in virus suspensions is presented. The anisotropy of the interactions experienced by a macromolecule is accounted for by a mean field potential, which is constructed as the superposition of short-range repulsions and long-range charge interactions. Despite the complexity of the system, these can be modeled in a simple way by virtue of the low macromolecular and virus concentration. The large asymmetry in charge and size of micro- and macroions present in the suspension is exploited to reduce the electrostatic problem to the determination of the effective electrostatic potential generated by the polyelectrolyte, with screening and renormalization parameters defined in terms of micro-ion charges and densities.[26] Steric repulsions are represented in terms of excluded volume between macromolecule and virion, both pictured as hard bodies, whereas electrostatic effects are described as Coulomb interactions between the macromolecular charges and the electrostatic potential experienced in the suspension. The electrostatic potential is calculated according to the Poisson−Boltzmann theory; thus polarization of the solvent and of the mobile ions are simply included in terms of dielectric constant and ion density. The virus is sketched as an infinitely long cylinder with a homogeneous charge density on its surface. On the contrary, the three-dimensional structure and charge distribution of the macromolecule are represented with atomistic detail.[33] In substance, the methodology relies on the same assumptions, which are at the basis of theories for orientational order in suspensions of charged rods. These date back to the paper of Onsager, who first demonstrated the existence of the isotropic−nematic transition in dilute solutions of long rods.[35] Such a theory and its subsequent modifications,

introduced to account for the rod flexibility[36] or to improve the description of electrostatic or concentration effects,[37,38] have been shown to be able to capture the essential physics of the problem. In principle, the effectiveness of this kind of description to model the alignment of solutes such as proteins cannot be taken for granted, given the subtle role played in this case by the molecular shape and charge distribution.

In the following the model for alignment of macromolecules in dilute nematic suspensions of viruses will be presented; then application to the prediction of $^{15}N-^{1}H$ residual dipolar couplings of protein G will be considered, and the results will be compared with the available experimental data.

Modeling of Order in Virus Suspensions

Orientational Mean Field. The anisotropic interactions of a macromolecule in an oriented virus suspension are accounted for by a mean field potential, $U^{mf}(\omega)$, where $\omega = (\theta,\varphi)$ are the angles defining the molecular orientation in the laboratory frame, taken with the Z axis parallel to the C_∞ symmetry axis of the suspension (the nematic director). The mean field is related to the orientational distribution function $f(\omega)$ of the macromolecule

$$f(\omega) = \frac{\exp[-U^{mf}(\omega)/k_B T]}{Q} \tag{1}$$

where T is the temperature, k_B is the Boltzmann constant, and Q is the orientational partition function

$$Q = \int d\omega \exp[-U^{mf}(\omega)/k_B T] \tag{2}$$

The interactions between macromolecules and virions can be characterized as short-range repulsions, which prevent the particles from overlapping, and longer range electrostatic interactions involving their charge distributions. Accordingly, the mean field will be expressed as the superposition of two contributions:

$$U^{mf} = U^{mf}_{hb} + U^{mf}_{el} \tag{3}$$

The term U^{mf}_{hb} will be modeled on the basis of hard body interactions. In view of the low virus and macromolecule concentration, the contribution of these to the free energy of the system can be approximated by the second term of the virial expansion.[39] Accordingly, the mean field experienced by a macromolecule will be expressed in terms of the volume excluded to it by a viral particle, averaged over the orientational distribution function of the virus:

$$U^{mf}_{hb}(\omega) = \frac{k_B T}{\upsilon_v}\int d\omega_v f_v(\omega_v)\upsilon_{excl}(\omega') \tag{4}$$

where the index υ is used to refer to virus. In particular, $\upsilon_v = V/N_v$ is the volume per virion, V and N_v being the total volume and the number of viral particles, $f_v(\omega_v)$ is the orientational distribution function of the virus, and $\omega_v = (\theta_v,\varphi_v)$ are the angles specifying the virus orientation in the laboratory frame. The excluded volume function is defined as the integral

$$\upsilon_{excl}(\omega') = -\int dr'\, \Theta(r',\omega') \tag{5}$$

with the step function

$$\Theta(r',\omega') = \begin{cases} -1 & \text{for macromol.} - \text{virus} \quad \text{overlapping} \\ 0 & \text{nonoverlapping} \end{cases} \tag{6}$$

and the variables (r',ω') defining respectively the mutual position and orientation of virion and macromolecule. The various reference frames and the corresponding transformations are summarized in Scheme 1.

SCHEME 1: Reference Frames and Transformations among Them

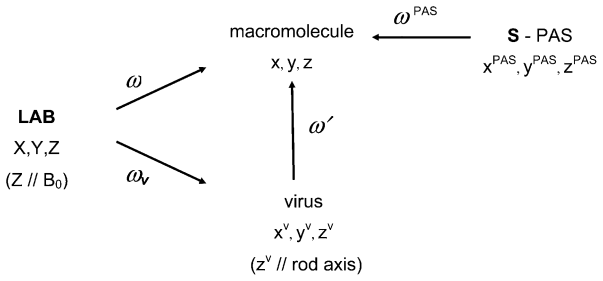

The representation of the electrostatic contribution to the orienting mean field is in principle less straightforward, because the electrostatic interactions between virions and macromolecules in the suspension are mediated by the solvent and the dissolved ions (which exist even in the absence of salt, because of the polyelectrolite nature of viruses). However, a simple mean field description based on the averaged Coulomb interaction between a macromolecule and a screened viral particle can be appropriate, by virtue of the properties of the system, i.e., small macromolecular concentration, high asymmetry between macromolecules or microions and poyelectrolytes, and orientational order of the suspension. Thus, we can write for the electrostatic contribution to the orientational mean field:

$$U^{mf}_{el}(\omega) = \frac{1}{\upsilon_v}\int d\omega_v f_v(\omega_v) \int dr'\, U^{el}(r',\omega')\, g_{hb}(r',\omega') \tag{7}$$

where g_{hb} is the hard body pair correlation function between a macromolecule and a viral particle, which for the sake of simplicity is assumed to have the form of a step function,

$$g_{hb}(r',\omega') = \begin{cases} -1 & \text{for macromol.} - \text{virus} \quad \text{overlapping} \\ 0 & \text{nonoverlapping} \end{cases} \tag{8}$$

and $U^{el}(\boldsymbol{r}',\omega')$ is the Coulomb interaction between the molecular charges and the effective electrostatic potential Ψ generated by the screened virus, when the macromolecule is in the orientation ω' and has its center of mass in r' (expressed in the virus frame). If the charge distribution of the macromolecule is approximated as a sum of discrete charges, we can write:

$$U^{el}(r',\omega') = \sum_j q_j \Psi(r'_j) \tag{9}$$

where $\Psi(r'_j)$ is the electrostatic potential at the position of the charge q_j, which is calculated by solving the Poisson−Boltzmann equation, as explained below.

In analogy with eq 5 we shall introduce the function

$$u_{el}(\omega') = \int dr'\, U^{el}(r',\omega')\, g_{hb}(r',\omega') \tag{10}$$

so that eq 7 can be expressed in the more compact form

$$U^{mf}_{el}(\omega) = \frac{1}{\upsilon_v}\int d\omega_v f_v(\omega_v)\, u_{el}(\omega') \tag{11}$$

Both the excluded volume υ_{excl} and the electrostatic contribution u_{el} depend on the orientation of the macromolecule, if this has anisometric shape and anisotropic charge distribution. In the case of a prolate macromolecule the excluded volume is minimized when the long axis is parallel to the director, whereas

in the case of an oblate particle the smallest excluded volume values correspond to orientations with the short axis perpendicular to the director. The electrostatic contribution takes its lowest values for orientations that allow positively (negatively) charged groups to lie closer to (farther from) the negatively charged virus surface.

Poisson−Boltzmann Theory for a Charged Rod with Added Salt. Let us consider a virus suspension in water, in the presence of counterions and salt. The *m* microions have charge z_m (in electron units) and average number density n_m^0. Within the cell approach,[40−43] which is reasonable for the liquid crystal phases of colloidal dispersions, attention can be restricted to the problem of a polyion at the center of a finite volume containing its own ion cloud and having zero net charge. Dimension and geometry of the cell reflect concentration and shape of the virus. The electrostatic potential Ψ in the cell can then be evaluated by solving the Poisson−Boltzmann equation, which relies on a mean-field description of the microion distribution. In the case of our rod-shaped viral particles the polyion can be approximated as an infinitely long cylinder, in the presence of counterions and added salt. So a cylindrical cell, coaxial with the rod, is appropriate and the cylindrically symmetric electrostatic potential Ψ is the solution of the (nonlinear) Poisson−Boltzmann equation:

$$\frac{d^2\Psi(r')}{dr'^2} + \frac{1}{r'}\frac{d\Psi(r')}{dr'} = -\frac{e}{\epsilon_0\epsilon}\sum_m z_m n_m(r') \tag{12}$$

where e is the electron charge and ϵ is the (relative) dielectric permittivity of the solvent (water). The ion density n_m is a function of the distance from the cylinder:

$$n_m(r') = n_m^0 \frac{e^{-z_m\Psi(r')e/k_BT}}{\frac{2}{(R_c - r_c)^2}\int_{r_c}^{R_c} dr'\, r' e^{-z_m\Psi(r')e/k_BT}} \tag{13}$$

where r_c and R_c are the radius of the rod and that of the cell. Appropriate boundary conditions involve the electric field on the surface of the polyion and at the boundary of the cell:

$$\begin{cases} \left(\frac{\partial\Psi(r')}{\partial r'}\right)_{r'=r_c} = -\frac{e}{2\pi\epsilon\epsilon_0\lambda r_c} \\ \left(\frac{\partial\Psi(r')}{\partial r'}\right)_{r'=R_c} = 0 \end{cases} \tag{14}$$

where λ is the linear charge density (in electron per unit length). If this is sufficiently low, the linear Debye−Hückel equation is recovered, which has an analytical solution. However this is not the case for viruses; therefore the problem has to be solved numerically.

Macromolecular Alignment and Residual Dipolar Couplings. The residual dipolar coupling (in Hz) between the P and Q nuclei connected by the vector $\mathbf{r}_{PQ}$ in a macromolecule dissolved in a nematic virus suspension ($\Delta\chi > 0$) can be expressed as

$$D_{PQ} = -\frac{\mu_0 h}{16\pi^3}\gamma_P\gamma_Q\langle r_{PQ}^{-3}\rangle_v S'_{PQ}\sum_{i=x,y,z}\cos^2\phi_i S_{ii} \tag{15}$$

where γ_P, γ_Q are the gyromagnetic ratios of the two nuclei, $\langle r_{PQ}^{-3}\rangle_v$ is the vibrationally averaged inverse cube of the distance between the nuclei, h and μ_0 are respectively the Planck constant and the vacuum magnetic permeability, and S'_{PQ} is the order parameter accounting for fluctuations of the internuclear vector around its average orientations in the molecular frame. In the absence of large amplitude P−Q reorientations, like those deriving from conformational changes, we can assume $S'_{PQ} \sim 1$. Therefore the product of factors multiplying the summation is practically a constant. On the contrary, the summation $\sum_{i=x,y,z}\cos^2\phi_i S_{ii}$, where S_{ii} is the ith principal value of the Saupe ordering matrix[35] and ϕ_i is the angle between the P−Q bond and the ith principal axis of S, depends on the alignment and conformation of the macromolecule (see Appendix A for the derivation of eq 15 and a few comments on it, and appendix B for the properties of the Saupe matrix). If dipolar couplings are measured in aligning media differing for the nature of the colloidal costituents or the physicochemical conditions, e.g., pH or salt content, as long as the molecular conformation is not affected by the environment, the change in D_{PQ} profile reflects the change in the values and axes of the Saupe tensor, i.e., in the alignment of the macromolecule.

The elements of the Saupe matrix are defined as the following averages over the orientational distribution function of the macromolecule in the ordered suspension:

$$S_{ij} = \frac{1}{Q}\int d\omega\,\frac{3\cos\theta_i\cos\theta_j - \delta_{ij}}{2}\exp[-U^{mf}(\omega)/k_BT] \tag{16}$$

where θ_i denotes the angle between the i axis of the macromolecular frame and the Z laboratory axis.

The mean field U^{mf} is made of an isotropic part (U_0^{mf}), which would be experienced in the liquid phase, and an anisotropic correction (ΔU^{mf}), which is different from zero in the liquid crystal phase. In weakly ordered virus suspensions $\Delta U^{mf}/k_BT \ll 1$ holds; therefore the Taylor expansion of the exponential with respect to the anisotropic correction can be truncated at the first-order term:

$$\exp[-U^{mf}(\omega)/k_BT] \approx \exp[-U_0^{mf}/k_BT]\left\{1 - \frac{\Delta U^{mf}(\omega)}{k_BT}\right\} \tag{17}$$

whereas the orientational partition function Q can be approximated by its value in the isotropic phase $Q \approx Q_0 = 4\pi\exp[-U_0^{mf}/k_BT]$. By using these relations and introducing the expressions for the steric and electrostatic contributions, eqs 4 and 11, after some algebraic manipulation (see Appendix C), we can rewrite eq 16 as

$$S_{ij} = -\frac{1}{4\pi v_v}S_v\int d\omega'\,\frac{3\cos\theta'_i\cos\theta'_j - \delta_{ij}}{2}\times \left[v_{excl}(\omega') + \frac{1}{k_BT}u_{el}(\omega')\right] \tag{18}$$

where θ'_i is the angle between the i macromolecular axis and the z_v axis in the virus frame and S_v is the orientational order parameter of the virus. This is the expression to be used to evaluate the alignment tensor of the macromolecule. We can see that it is the sum of a steric and an electrostatic term, with different temperature dependencies, calculated by integrating respectively excluded volume and screened Coulomb interactions over all possible positions and orientations of the macromolecule in the virus frame. The weight of each contribution will depend on the experimental conditions; e.g., the relevance of the electrostatic term can be expected to decrease with increasing ionic strength, as a consequence of the increased screening of charge interactions between macromolecule and

virus. According to eq 18 the Saupe matrix scales linearly with the virus concentration N_v/V and the virus order parameter S_v; therefore the shape of the D_{PQ} profiles is predicted to remain practically the same when the virus content is changed.

Numerical Methods. The alignment tensor of the macromolecule is evaluated according to eq 18; excluded volume and average electrostatic interactions, eqs 5 and 10, are calculated as a function of the macromolecular orientation ω' in the virus frame by integrating over the vector $\mathbf{r}'$ joining the center of mass of the protein to the axis of the cylinder representing the viral particle. Integration is performed over the volume region contained in a cylinder of radius R_c, coaxial with the rod. In practice, for a given vector $\mathbf{r}'$ there is a contribution either to the excluded volume or to the average electrostatic interaction, according to whether the overlap condition between virion and macromolecule is satisfied or not. The two particles are assumed to overlap if at least one atom lies at a distance which is closer than $r_c^0 = r_c + 0.15$ nm from the axis of the cylinder. So, the steric and electrostatic contributions to eq 18 are calculated as

$$\frac{v_{excl}(\omega')}{v_v} = \frac{1}{\pi R_c^2}\left\{\pi r_c^2 + \int_{r_c}^{R_c} dr'\, r' \int_0^{2\pi} d\Phi'\, \Theta(r',\Phi',\omega')\right\} \quad (19)$$

and

$$\frac{u_{el}(\omega')}{v_v k_B T} = \frac{1}{\pi R_c^2}\sum_j z_j^M \int_{r_c}^{R_c} dr'\, r' \int_0^{2\pi} d\Phi'\, y(r_j')\, g_{hb}(r',\Phi',\omega') \quad (20)$$

with the macromolecular partial charges z_j^M (in electron units) and the scaled potential $y(r') = e\Psi(r')/k_BT$. No analytical solution of the Poisson−Boltzmann equation is available for the general case of nonzero salt concentration; therefore the scaled potential is obtained numerically, by using the Newton method. Because the ion density $n_m(r')$ depends on the electrostatic potential (see eq 13), an iterative procedure is used.

Calculation of the reduced dipolar couplings is very fast, requiring only a few minutes on a desktop computer; this feature would be important for the use of the methodology presented here for the analysis of NMR experiments.

Application: Residual $^1D_{NH}$ Dipolar Couplings of Protein G

The model presented above has been used to predict the NH residual dipolar couplings of the Ig-binding domain of Streptococcal protein G in a dilute nematic suspension of the filamentous bacteriophages *fd*, Pf1, and TMV. The characteristics of the three viruses are listed in Table 1. For the calculation of excluded volume and average Coulomb interactions, eqs 5 and 10, viruses have been modeled as infinitely long cylinders of radius r_c with homogeneously distributed charge over their surface. The protein geometry has been taken from the X-ray structure[45] (entry code 1IGD in the Brookhaven Protein Data Bank[46]), shortened by five residues at the N-terminus, as in the system for which measurements of NH dipolar couplings have been reported.[13] In this way the model protein has 56 residues. Hydrogen atoms have been neglected in the calculations, with the exception of hydrogens bearing charges, which have been added with the Hyperchem package.[47] Protein charges for the calculation of the screened Coulomb interactions eq 9 have been introduced according to the Gromacs parametrization: in this way partial charges are assigned to the NH and CO groups of all residues, beside other additional partial charges in some of the C_α substituents.[48] With pH values higher than 5 and lower than 9, the protonated and the deprotonated state has been assumed respectively for Lys and N-term, and for Glu, Asp, and C-term, respectively. In this way the total molecular charge amounts to $-2e$. Figure 2 shows the electrostatic potential generated by the molecular charge distribution on the protein surface, with the strong blue and red colors corresponding respectively to positively and negatively charged residues. In all calculations reported below $T = 300$ K and $\epsilon = 80$ have been taken.

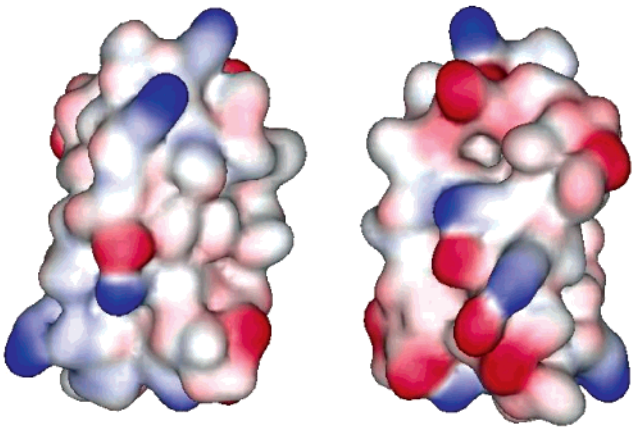

Figure 2. Two-side view of the electrostatic potential on the molecular surface of the protein G, with red and blue corresponding respectively to negative and positive values (represented with ViewerPro[49]). The more strongly colored regions correspond to charged residues (Glu, Asp, Lys).

TABLE 2: Largest Principal Value and Rhombicity of the Saupe Ordering Matrix, Together with the Euler Angles for the Rotation from the PAS of the Saupe Matrix to the Original Molecular Frame, Predicted for the G Protein in a Nematic Virus Suspension under Different Conditions[a]

	S_{zz}	R	α^{PAS}/deg[e]	β^{PAS}/deg[e]	γ^{PAS}/deg[e]	ψ/deg
b	0.00047	0.24	73	90	178	0
600 mM[c]	0.00035	0.55	77	118	153	37
d	0.00032	0.58	82	118	149	39
100 mM[c]	0.00103	0.55	110	89	121	57
d	0.00121	0.69	112	80	110	68
50 mM[c]	0.00148	0.64	112	82	114	64
d	0.00169	0.75	113	78	108	70
20 mM[c]	0.00203	0.75	113	78	108	70
d	0.00226	0.84	113	76	105	74
10 mM[c]	0.00242	0.83	113	76	105	74
d	0.00266	0.90	113	75	103	76

[a] The angle ψ defines the rotation from the main alignment axis (z^{PAS}) predicted in each case and the main alignment axis predicted in the presence of purely steric interactions. In the first column the concentration of added 1:1 salt is reported. [b] Purely steric interactions. [c] Steric and electrostatic interactions. [d] Purely electrostatic interactions. [e] Euler angles are defined according to the convention of ref 50:

$$(x^{PAS}, y^{PAS}, z^{PAS}) \xrightarrow{\alpha^{PAS}} (x_1, y_1, z_1 = z^{PAS}) \xrightarrow{\beta^{PAS}} (x_2, y_2 = y_1, z_2) \xrightarrow{\gamma^{PAS}} (x, y, z = z_2)\ \text{(counterclockwise rotations)}$$

Table 2 reports the largest principal value, S_{zz}, and the rhombicity R of the Saupe order matrix (see Appendix B), together with the Euler angles (α^{PAS}, β^{PAS}, γ^{PAS}) for the rotation from the PAS of the Saupe matrix to the original molecular frame (PDB coordinates). In the last column the angle ψ between the main alignment axis (z^{PAS}) and the alignment axis predicted for purely steric interactions is reported. In the calculations the value $R_c = 20$ nm has been chosen, which corresponds to a concentration $c_v \sim 30$ mg/mL for *fd* bacteriophage. Different concentrations of 1:1 added salt are considered,

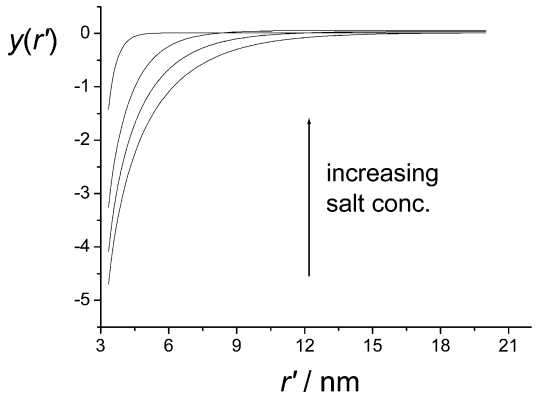

Figure 3. Scaled electrostatic potential $y(r') = e\Psi(r')/k_BT$, obtained by solving the cylindrical Poisson−Boltzmann equation for different ionic strengths, as a function of the distance from the axis of the infinitely long charged cylinder. From top to bottom the curves correspond to decreasing concentrations of 1:1 added salt (the values are 600, 50, 20, and 10 mM).

in addition to an amount of monovalent counterions sufficient to neutralize the virus charge (∼13 mM for a linear charge density $\lambda = -10$ *e*/nm). To better highlight the different contributions of steric and electrostatic interactions, also the results obtained by switching off the one or the other of them are reported in Table 2. It can be seen that the two kinds of interactions contribute quite differently to alignment of protein G, with substantial differences in both the principal values and the axes of the Saupe matrix. Focusing on the electrostatic contribution, we can see that addition of salt has the effect of reducing its magnitude, without substantially altering the predicted alignment directions of the macromolecule. The screening effect of salt, which tunes the length scale of the electrostatic interactions between macromolecule and virus, appears from Figure 3, where the decay of the electrostatic potential with distance from the viral particle is shown. We can see in Table 2 that, even though the macromolecule is not strongly charged, its orientational behavior is mainly driven by electrostatic interactions, at least if the salt concentrations is not extremely high.

Going now into more detail, we can see that the predicted angle between the main alignment axes for steric and electrostatic interactions is wider than 60°. Moreover, a pronounced difference in the biaxiality of order appears: the alignment tendency changes from rodlike ($R < 2/3$) in the case of steric interactions toward disklike ($R > 2/3$) when electrostatic contributions are considered. These results are in surprisingly good agreement with the experimental observations: a change in rhombicity from 0.23 to 0.66 has been reported on passing from bicelle virus suspensions, along with angles of about 80° between the principal *z* axes of the alignment tensors in the two cases.[13]

We can now analyze the effects on the measurable NMR quantities, i.e., the residual dipolar couplings. To this purpose it is convenient to introduce dimensionless residual dipolar couplings, defined as

$$d_{NH} = -(1/S_v)\sum_{i=x,y,z} \cos^2 \phi_i \, S_{ii} \qquad (21)$$

where S_{ii} is the *i*th diagonal element of the Saupe matrix of the macromolecule, see eq 18, and S_v is the orientational order parameter of the virus (see Appendix B). Comparison with eq 15 shows that the d_{NH} values are related to the experimental NH couplings by the scaling factor

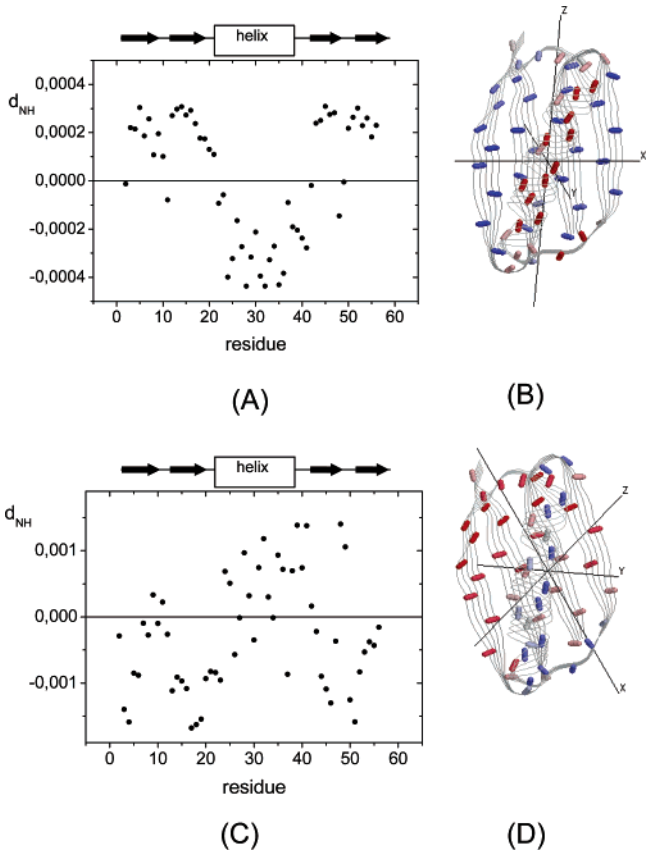

Figure 4. Scaled d_{NH} couplings calculated for only steric (A, B) and only electrostatic (C, D) interactions at 50 mM concentration of added salt. In parts B and D the principal frames (x^{PAS}, y^{PAS}, z^{PAS}) of the Saupe matrix are shown and the d_{NH} values are represented by the colors of the NH bonds along the protein backbone. The color code is such that the orientation of the NH bond changes from parallel to perpendicular to the magnetic field on going from red to blue, with colors normalized within each figure (represented with Rasmol[51]).

$c = (\mu_0 h/16\pi^3)\gamma_N\gamma_H\langle r_{NH}^{-3}\rangle_v S'_{NH} S_v$. A reasonable estimate, obtained with $S_v = 0.8$ and $\langle r_{NH}^{-3}\rangle_v S'_{NH} = 880$ nm^{-3},[27] is $c = -0.85 \times 10^4$ Hz. It follows from the definition that negative and positive d_{NH} values correspond to NH bonds respectively parallel and perpendicular to the nematic director (to the static magnetic field), with magnitude that decreases with the degree of alignment.

In Figure 4A,B the PAS of the Saupe matrix and the scaled residual dipolar couplings calculated under the assumption of purely steric alignment mechanism (first row of Table 2) are shown. As can be expected on the basis of the protein shape, steric interactions tend to align the long molecular axis, which is not far from the axis of the α-helix, to the nematic director (and then to the magnetic field). Such an alignment produces a d_{NH} pattern in which the NH bonds belonging to differently structured parts of the protein can be immediately distinguished: those in the β sheets are nearly perpendicular to the magnetic field, whereas those in the α helix are more aligned to it. The pattern reveals a clear resemblance to that reported in Figure 1A, where the $^1D_{NH}$ residual dipolar couplings measured in a neutral bicelle suspension are shown. Owing to the global negative charge of the protein, the electrostatic interactions between protein and virus are expected to have a repulsive character; however, in view of the complexity of the charge distribution in the protein shown in Figure 2, the angular dependence of such interactions, which is at the origin of electrostatic alignment, cannot be easily figured out. The results of our calculations, displayed in Figure 4C,D, indicate that the

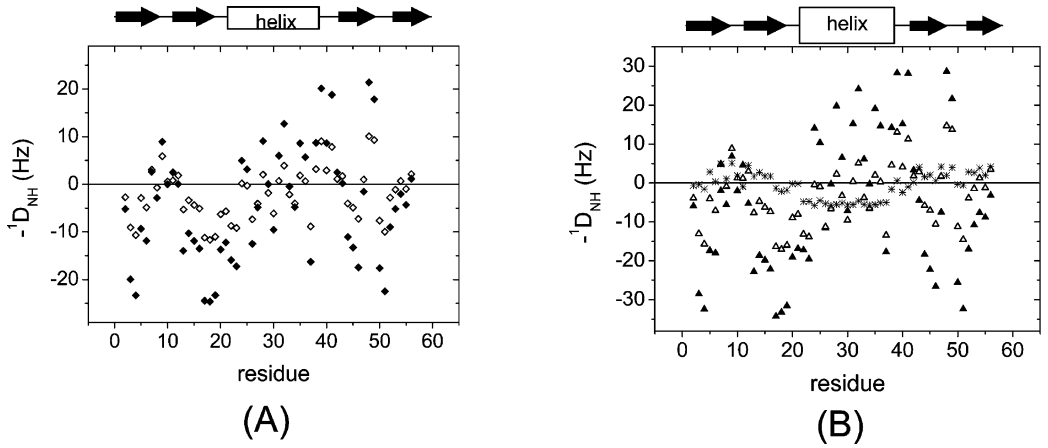

Figure 5. Residual dipolar couplings predicted for G protein in different conditions. (A) *fd* virus ~ 30 mg/mL (◆) and TMV ~ 50 mg/mL (◇), with 50 mM 1:1 added salt. (B) *fd* virus ~ 30 mg/mL, at different concentrations of 1:1 added salt: 600 mM (*), 100 mM (△), and 20 mM (▲).

axis preferentially aligned to the director (the z^{PAS} axis) is in this case nearly perpendicular to the long molecular axis; correspondingly, the d_{NH} pattern is completely different from that shown in Figure 4A, with most couplings that have changed their sign.

Finally, we can try a closer comparison with experimental data. The choices specified above for virus and cell radius and virus charge density are roughly appropriate for the *fd* suspensions considered in Figure 1B; in the case of TMV the values $r_c = 9$ nm, $R_c = 34$ nm and $\lambda = -20$ *e*/nm have been used. In all cases the scale factor c is given the value -0.85×10^4Hz, by neglecting its dependence on the degree of alignment of the phase. The agreement between theoretical calculations and experimental observations clearly appears from comparison of Figures 1B and 5A: the pattern is correctly predicted, as well as the magnitude of the dipolar couplings and the changes due to the virus dimension and concentration. Looking in more detail we can see that some larger discrepancies between calculated and measured $^1D_{NH}$ values appear at residues, e.g., 49 and 50, that are located in turns or unstructured parts of the protein. These are characterized by higher conformational mobility; therefore it is not surprising that for NH bonds belonging to such regions the residual couplings predicted on the basis of the crystal structure do not strictly correspond to those measured in solution.

Figure 5B shows the effect of ionic strength on the NH residual dipolar couplings. We can see that for 20 and 100 mM added salt similar patterns are obtained, although the magnitude of the splittings is predicted to decrease significantly with increasing ionic strength. On the contrary, a quite different $^1D_{NH}$ profile is obtained at 600 mM added salt, with a change of sign of the splitting at most residues; a resemblance with the data reported for neutral bicelle suspensions (see Figure 1A) clearly appears. The theoretical predictions are in agreement with experimental findings: both the lack of correlation between the $^1D_{NH}$ values at very different ionic strengths and the increase in magnitude of the dipolar couplings with decreasing salt concentration have been observed for G protein in Pf1 suspensions, as displayed in Figure 1C. For a less qualitative comparison one should scale the values reported in Figure 5B with a factor larger than the unity, to take into account that, at similar weight concentration, colloidal suspensions of Pf1 should be more ordered than those of *fd*.[36] So, the magnitude of the predicted dipolar couplings would be comparable with the experimental data reported in Figure 1C for 600 mM salt, whereas too large dipolar couplings would be predicted at very low ionic strength. Such a discrepancy might depend on our simple representation of electrostatic interactions, which would become less satisfactory when charges of virus and macromolecule are only weakly screened. Another possible reason, which probably cannot be ruled out, is the difficulty of controlling the actual salt concentration in virus suspensions at very low ionic strength.

Concluding Remarks

In this work a model for the steric and electrostatic origin of alignment of macromolecules in dilute nematic suspensions of filamentous viruses has been presented. The anisotropic orientational distribution of macromolecules is derived from a mean field potential, approximated in terms of the superposition of excluded volume and screened Coulomb interactions in water between a macromolecule and a viral particle. The virus is represented as an infinitely long rod with uniform charge distribution on its surface, whereas the details of the structure and charge distribution of the macromolecule are explicitly taken into account.

The model has been applied to calculation of $^{15}N-^1H$ residual dipolar couplings for Ig-binding domain of streptococcal protein G; this has been chosen as the test system because it has a stable structure, practically unaffected by changes of the environment, and for this molecule experimental data from NMR measurements in different alignment media are available in the literature. A variety of models for the anisotropy of steric repulsions, which is the only cause of alignment in neutral bicelle suspensions, have been reported in the past few years.[27−30] In this work it has been shown that also the prediction of the electrostatic contribution to alignment can be afforded with simple tools. This is a further step toward a better understanding of the behavior of macromolecules in dilute nematic suspensions, which can be useful for the interpretation of NMR experiments performed in such media. Application of this technique is rapidly growing, extending from determination of the three-dimensional structure biomolecules to the investigation of their internal dynamics[52] and the study of processes such as dimer formation and macromolecule-colloid association.[53,54]

A number of assumptions are taken in the present approach: the charge distribution in the macromolecule is represented in terms of partial charges, which are parametrized in a standard way; structure and charge inhomogeneity of the virus are neglected; polarization in the macromolecule and in the environment are not taken into account; the effects of the microions present in the suspension are introduced at the mean field level, through a cylindrical Poisson−Boltzmann equation for the rod-shaped virus. Nevertheless, the theoretical predictions for the

G protein, which is characterized by a complex structure and charge distribution, provide a sound explanation for the orientational behavior inferred from the $^{15}N-^{1}H$ residual dipolar couplings reported in the literature. This is somehow surprising, in view of the extreme sensitivity of such NMR observables to the features of the interactions between the specific macromolecule and its environment. The present approach, which has the advantage of a low computational cost, is potentially useful for the refinement of NMR structures. A more precise definition of the predictive capability of the model would require it to be tested on a wider class of systems. Extension of this approach to suspensions of other charged colloids of different shape can also be considered; in principle, the method should still be appropriate, provided that dilution is sufficiently high and the charge and shape features of the colloidal particles are known.

Acknowledgment. This work has been supported by MURST *PRIN Cristalli Liquidi* and EU *TMR* contract FMRX CT97 0121. I am grateful to prof. Giorgio Moro and dr. Massimo Bellanda for stimulating discussions.

Appendix A

Expression for the Residual Dipolar Couplings. The dipolar coupling (in Hz) between the two nuclei P and Q connected by the vector $\mathbf{r}_{PQ}$ is given by[1,2a]

$$D_{PQ} = -\frac{\mu_0 h}{16\pi^3}\gamma_P\gamma_Q\left\langle\frac{3\cos^2\theta_{PQ}-1}{2r_{PQ}^{\ 3}}\right\rangle \qquad \text{(A1)}$$

where γ_P, γ_Q are the gyromagnetic ratios of the two nuclei and θ_{PQ} is the angle between the applied magnetic field and the internuclear vector. The brackets denote the average over all orientations and lengths of such a vector, which are modulated by overall rotations of the molecule and intramolecular motions. If the nuclei P and Q are connected by a bond, the average over small-amplitude vibrational motions that affect the distance r_{PQ} can be assumed to be independent of reorientations of the internuclear vector; therefore we can write

$$D_{PQ} = -\frac{\mu_0 h}{16\pi^3}\gamma_P\gamma_Q\langle r_{PQ}^{\ -3}\rangle_v S_{PQ} \qquad \text{(A2)}$$

where $\langle\ \rangle_v$ denotes a vibrational average and $S_{PQ} = \langle(3\cos^2\theta_{PQ}-1)/2\rangle$ accounts for the alignment of the internuclear vector with the applied magnetic field. In this term we can distinguish the contributions from reorientations of the internuclear vector in the molecular frame and from overall reorientations of the molecule; if axial symmetry is assumed for the former, we can write $S_{PQ} = S'_{PQ}\,S''_{PQ}$, where S'_{PQ} and S''_{PQ} are order parameters for the fluctuations of the internuclear vector about its average orientation in the molecular frame and for those of the average internuclear vector with respect to the applied magnetic field, respectively. Finally, it is customary to express S''_{PQ} in terms of the orientation of the average internuclear vector in the molecular frame and of the Saupe ordering matrix **S** of the molecule,[44] which describes the alignment of the molecular axes with the nematic director (see Appendix B). In virus suspensions ($\Delta\chi > 0$) the director aligns parallel to the applied magnetic field; therefore the dipolar coupling between nuclei P and Q can then be expressed as[3]

$$D_{PQ} = -\frac{\mu_0 h}{16\pi^3}\gamma_P\gamma_Q\langle r_{PQ}^{\ -3}\rangle S'_{PQ}\sum_{i=x,y,z}\cos^2\phi_i S_{ii} \qquad \text{(A3)}$$

where S_{ii} is the ith principal value of the Saupe ordering matrix and ϕ_i is the angle between the P−Q bond and such an axis. Let us consider now a macromolecule with several pairs of PQ interacting nuclei: the vibrational average $\langle r_{PQ}^{\ -3}\rangle$ is very similar for all pairs and, in the absence of large amplitude intramolecular motions, also the local order parameter S'_{PQ} can be assumed to be independent of the position ($S'_{PQ} \sim 1$ in most cases). Therefore the residual dipolar couplings measured at different positions essentially depend on the average orientation of the P−Q bonds in the molecular frame, i.e., on the molecular conformation. This is the basis of the use of residual magnetic couplings for structure determination of macromolecules. Let us assume that the molecular conformation does not change when the macromolecule is dissolved in different aligning media; nevertheless, both the magnitude and the principal axes of the Saupe matrix **S** can change as a consequence of the change in intermolecular interactions, and this results in a change of the D_{PQ} profile.

Appendix B

The Saupe Matrix. The elements of the Saupe matrix, which specify the alignment of a molecule in a uniaxial phase, are defined as

$$S_{ij} = \int d\omega\,\frac{3\cos\theta_i\cos\theta_j - \delta_{ij}}{2}f(\omega) \qquad \text{(B1)}$$

where θ_i is the angle between the i molecular axis and the C_∞ symmetry axis of the phase (the director in nematics) and $f(\omega)$ is the orientational distribution function of the molecule, ω being the set of angles that define its orientation. It can be easily shown, by using trigonometry relations, that the Saupe matrix is symmetric ($S_{ij} = S_{ji}$), traceless ($S_{xx} + S_{yy} + S_{zz} = 0$), and $-(1/2) < S_{ii} < 1$. In the principal axis system (PAS) of the matrix there are only two independent parameters; it is customary to choose the largest (positive) eigenvalue (denoted as S_{zz}) and the difference of the other eigenvalues, $S_{xx} - S_{yy}$. The latter is often replaced by the biaxiality $\lambda = (S_{xx} - S_{yy})/\sqrt{6}S_{zz}$, or by the rhombicity, which is defined as $R = 2(S_{xx} - S_{yy})/3S_{zz}$, with the labels x and y assigned in such a way that $S_{xx} - S_{yy} > 0$. It is worth remembering that the eigenvalue of the Saupe matrix with the largest absolute value is S_{zz} when $R < {}^2/_3$ and S_{yy} when $R > {}^2/_3$. By convention the orientational behavior of the molecule is defined respectively as rodlike and disklike in the two cases; a perfect rod and a perfect disk correspond respectively to $R = 0$ ($S_{xx} = S_{yy} = -S_{zz}/2$) and $R = 2$ ($S_{xx} = S_{zz} = -S_{yy}/2$).

Appendix C

Derivation of Equation 18. After substitution of eq 17 into eq 16, we can write

$$S_{ij} = -\frac{1}{k_B T}\frac{3}{2}\int d\omega\,\cos\theta_i\cos\theta_j\Delta U^{mf}(\omega) \qquad \text{(C1)}$$

By introducing now the expressions for the steric and electrostatic contributions, eqs 4 and 11, and recalling that the ΔU^{mf} is the difference between the mean field potential in the nematic and in the liquid phase (where $f_v(\omega) = 1/4\pi$), we obtain the following expression:

$$S_{ij} = -\frac{1}{4\pi v_v}\frac{3}{2}\int d\omega\,\cos\theta_i\cos\theta_j\int d\omega_v\left[f_v(\omega_v) - \frac{1}{4\pi}\right]\times \left\{v_{excl}(\omega') + \frac{1}{k_B T}u_{el}(\omega')\right\} \qquad \text{(C2)}$$

Equation B2 can be simplified if the transformation from the laboratory to the molecular frame is decomposed into the rotation from the laboratory to the virus frame, followed by a rotation from the virus to the macromolecular frame: $\cos\theta_i = \sum_k \cos\theta'_{ik}\cos\theta^{\mathrm{v}}_k$, where θ'_{ik} is the angle between the i axis in the macromolecular frame and the k axis in the virus frame and θ^{v}_k is the angle between the k axis in the latter frame and the Z laboratory axis. Thus

$$S_{ij} = -\frac{1}{4\pi v_{\mathrm{v}}}\frac{3}{2}\sum_{k,l}\int \mathrm{d}\omega_{\mathrm{v}}\left[f_{\mathrm{v}}(\omega_{\mathrm{v}}) - \frac{1}{4\pi}\right]\times \cos\theta^{\mathrm{v}}_k\cos\theta^{\mathrm{v}}_l\int \mathrm{d}\omega'\cos\theta'_{ik}\cos\theta'_{jl}\left\{v_{\mathrm{excl}}(\omega') + \frac{1}{k_{\mathrm{B}}T}u_{\mathrm{el}}(\omega')\right\} \quad \text{(C3)}$$

where the two integrals, respectively over the virus and the macromolecular distribution, are factorized. Because viruses used for aligning media can be pictured as rods, we can write

$$\int \mathrm{d}\omega_{\mathrm{v}} f_{\mathrm{v}}(\omega_{\mathrm{v}})\cos\theta^{\mathrm{v}}_k\cos\theta^{\mathrm{v}}_l = \delta_{l,k}\left[\frac{1}{3} + \frac{2}{3}S_{\mathrm{v}}\left(\delta_{k,z} - \frac{1}{2}\delta_{k,x} - \frac{1}{2}\delta_{k,y}\right)\right] \quad \text{(C4)}$$

$$\int \mathrm{d}\omega_{\mathrm{v}}\cos\theta^{\mathrm{v}}_k\cos\theta^{\mathrm{v}}_l = \frac{4\pi}{3}\delta_{l,k} \quad \text{(C4')}$$

where S_{v} is the orientational order parameter of the virus, $S_{\mathrm{v}} = \int \mathrm{d}\omega_{\mathrm{v}} f_{\mathrm{v}}(\omega_{\mathrm{v}})(3\cos^2\theta^{\mathrm{v}}_z - 1)/2$, and $\delta_{i,j}$ is the Kronecker symbol. Moreover, by virtue of the axial symmetry of the virus, in the virus frame we can write

$$\int \mathrm{d}\omega'\cos\theta'_{ik}\cos\theta'_{jk}\left\{v_{\mathrm{excl}}(\omega') + \frac{1}{k_{\mathrm{B}}T}u_{\mathrm{el}}(\omega')\right\} = \left(\delta_{k,z} - \frac{1}{2}\delta_{k,x} - \frac{1}{2}\delta_{k,y}\right)\int \mathrm{d}\omega'\cos\theta'_{iz}\cos\theta'_{jz}\times \left\{v_{\mathrm{excl}}(\omega') + \frac{1}{k_{\mathrm{B}}T}u_{\mathrm{el}}(\omega')\right\} + \left(\frac{1}{2}\delta_{k,x} + \frac{1}{2}\delta_{k,y}\right)\int \mathrm{d}\omega'\left\{v_{\mathrm{excl}}(\omega') + \frac{1}{k_{\mathrm{B}}T}u_{\mathrm{el}}(\omega')\right\} \quad \text{(C5)}$$

By making use of eqs C4−C4′ and C5, the expression for the elements of the Saupe matrix, eq 18, is obtained from eq C3.

References and Notes

(1) *Nuclear Magnetic Resonance of Liquid Crystals*; Emsley, J. W., Ed.; Reidel: Dordrecht, The Netherlands, 1985.

(2) (a) Khetrapal, C. L.; Nagana Gowda, G. A. In *NMR of Ordered Liquids*; Burnell, E. E., de Lange, C. A., Eds.; Kluwer: Dordrecht, The Netherlands (in press). (b) Celebre, G.; Longeri, M. In *NMR of Ordered Liquids*; Burnell, E. E., de Lange, C. A., Eds.; Kluwer: Dordrecht, The Netherlands (in press).

(3) Tjandra, N.; Bax, A. *Science* **1997**, *278*, 1111 and 1697 (erratum).

(4) Ramirez, B. E.; Bax, A. *J. Am. Chem. Soc.* **1998**, *120*, 9106.

(5) Prestegard, J. H.; Al-Hashimi, H. M.; Tolman, J. R. *Q. Rev. Biophys.* **2000**, *33*, 371.

(6) Tjandra, N.; Tate, S.; Ono, A.; Kainosho, M.; Bax, A. *J. Am. Chem. Soc.* **2000**, *122*, 6190.

(7) Al-Hashimi, H. M.; Majumdar, A.; Gorin, A.; Kettani, A.; Skripkin, E.; Patel, D. J. *J. Am. Chem. Soc.* **2001**, *123*, 633.

(8) Ian, F.; Al-Hashimi, H. M.; Craighead, J. L.; Prestegard, J. H. *J. Am. Chem. Soc.* **2001**, *123*, 485.

(9) Almond, A.; Bunkerborg, J.; Franch, T.; Gotfredsen, C. H.; Duus, J. Ø. *J. Am. Chem. Soc.* **2001**, *123*, 4792.

(10) Trempe, J.-F.; Gehring, K. In *NMR of Ordered Liquids*; Burnell, E. E., de Lange, C. A., Eds.; Kluwer: Dordrecht, The Netherlands (in press).

(11) Sanders, C. R.; Schwonek, J. P. *Biochemistry* **1992**, *31*, 8898.

(12) Hansen, M. R.; Mueller, L.; Pardi, A. *Nature Struct. Biol.* **1998**, *5*, 1065.

(13) Clore, G. M.; Starich, M. R.; Gronenborn, A. M. *J. Am. Chem. Soc.* **1998**, *120*, 10571.

(14) Zweckstetter, M.; Bax, A. *J. Biomol. NMR* **2001**, *20*, 365.

(15) Koenig, B. W.; Hu, J. S.; Ottiger, M.; Bose, S.; Hendler, R. W.; Bax, A. *J. Am. Chem. Soc.* **1999**, *121*, 1385.

(16) Sass, J.; Cordier, F.; Hoffmann, A.; Rogowski, M.; Cousin, A.; Omichinski, G. J.; Löwen, H.; Grzesiek, S. *J. Am. Chem. Soc.* **1999**, *121*, 2047.

(17) Al-Hashimi, H. M.; Valafar, H.; Terrel, M.; Zartler, e. R.; Eidsness, M. K.; Prestegard, J. H. *J. Magn. Reson.* **2000**, *295*, 1265.

(18) Peti, W.; Meiler, J.; Brüschweiler, R.; Griesinger, C. *J. Am. Chem. Soc.* **2002**, *124*, 5822.

(19) Losonczi, J. A.; Prestegard, J. H. *J. Biomol. NMR* **1998**, *12*, 447.

(20) Newman, J.; Swinney, H, L.; Day, L. A. *J. Mol. Biol.* **1977**, *116*, 593.

(21) Zimmermann, K.; Hagedorn, J.; Heuch, C. C.; Hinrichsen, M.; Ludwig, J. *J. Biol. Chem.* **1986**, *261*, 1653.

(22) Fraden, S. In *Observation, Prediction and Simulation of Phase Transition in Complex Fluids*; Baus, M., Ryckaert, J. P., Eds.; Kluwer: Dordrecht, The Netherlands, 1995.

(23) Hill, D. F.; Short, N. J.; Perham, R. N.; Petersen, G. B. *J. Mol. Biol.* **1991**, *218*, 349. Nambudripad, R.; Stark, W.; Makowski, L. *J. Mol. Biol.* **1991**, *220*, 359.

(24) Scheele, R. B.; Lauffer, M. A. *Biochemistry* **1967**, *6*, 3076.

(25) Purdy, K. R.; Dogic, Z.; Fraden, S.; Rühm, A.; Lurio, L.; Mochrie, S. G. *Phys. Rev. E* **2003**, *67*, 031708.

(26) Hansen, J. P.; Löwen, H. *Annu. Rev. Phys. Chem.* **2000**, *51*, 209.

(27) Zweckstetter, M.; Bax, A. *J. Am. Chem. Soc.* **2000**, *122*, 3791.

(28) Almond, A.; Axelsen, J. *J. Am. Chem. Soc.* **2002**, *124*, 9986.

(29) Azurmendi, H. F.; Allen Bush, C. *J. Am. Chem. Soc.* **2002**, *124*, 2426.

(30) Fernandes, M. X.; Bernadó, P.; Pons, M.; Garcia de la Torre, J. *J. Am. Chem. Soc.* **2000**, *120*, 12037.

(31) Ferrarini, A. Unpublished results.

(32) Ferrarini, A.; Moro, G. J.; Nordio, P. L.; Luckhurst, G. R. *Mol. Phys.* **1992**, *77*, 1; Ferrarini, A.; Janssen, F.; Moro, G. J.; Nordio, P. L. *Liq. Cryst.* **1999**, *26*, 201.

(33) It is worth remarking here that the model for steric interactions essentially coincides with that described by Zweckstetter and Bax,[14] and implemented in the routines of the PALES software package.[34]

(34) spin.niddk.nih.gov/bax/software/PALES.

(35) Onsager, L. *Ann. N. Y. Acad. Sci.* **1949**, *51*, 627.

(36) Khoklov, A. R.; Semenov, A. N. *Physica A* **1982**, *112*, 605.

(37) Stroobants, A.; Lekkerkerker, H. N. W.; Odijk, T. *Macromolecules* **1986**, *19*, 2232.

(38) Sato, T.; Teramoto, A. *Physica A* **1991,** *176*, 72.

(39) Hansen, J. P.; McDonald, I. R. *Theory of Simple Liquids*; Academic Press: London, 1986.

(40) Fuoss, R. M.; Katchalsky, A.; Lifson, S. *Proc. Natl. Acad. Sci. U.S.A.* **1951**, *37*, 579. Alfrey, T., Jr.; Berg, P. W.; Morawetz, H. *J. Polym. Sci.* **1951**, *7*, 543. Katchalski, A. *Pure Appl. Chem.* **1971**, *26*, 327.

(41) Löwen, H. *J. Chem. Phys.* **1994**, *100*, 6738.

(42) Deserno, M.; Holm, C.; May, S. *Macromolecules* **2000**, *33*, 199.

(43) Das, T.; Bratko, D.; Bhuiyan, L. B.; Outhwaite, C. W. *J. Phys. Chem.* **1995**, *99*, 410.

(44) Saupe, A. *Z. Naturforsch.* **1964**, *19a*, 161.

(45) Derrick, J. P.; Wigley, D. B. *J. Mol. Biol.* **1994**, *243*, 906.

(46) www.rcsb.org/pdb.

(47) Hyperchem Vers. 6.02; Hypercube: Gainesville, FL, 2000.

(48) van der Spoel, D.; van Buuren, A. R.; Apol, E.; Meulenhoff, P. J.; Tieleman, D. P.; Sijbers, A. L. T. M.; van Drunnen, R.; Berendsen, H. J. C. *Gromacs User Manual*; University of Groningen; Groningen, 1996.

(49) Accelerys ViewerPro Trial Edition Vers. 5.0; Accelerys Inc.: Cambridge, U.K., 2002.

(50) Zare, N. R. *Angular Momentum*; Wiley and Sons: New York, 1987.

(51) www.umass.edu/microbio/rasmol.

(52) Tolman, J. R.; Al-Hashimi, H. M.; Kay, L. E.; Prestegard, J. H. *J. Am. Chem. Soc.* **2001**, *123*, 1416.

(53) Meiler, J.; Prompers, J. J.; Peti, W.; Griesinger, C.; Brüschweiler, R. *J. Am. Chem. Soc.* **2001**, *123*, 6098.

(54) van Lune, F.; Manning, L.; Dijskra, K.; Berendsen, H. J. C.; Scheek, R. M. *J. Biomol. NMR* **2002**, *23*, 169.